01-11-SRJ-209-54

SIAZGA RESEARCH JOURNAL, 2024
VOL. 03, NO. 02, .96 – 105
DOI: https://doi.org/10.58341/srj.v3i2.54


Original Article

# A Comprehensive Tutorial on Graphene Family X-ray Diffraction Analysis: Graphical Representation of Miller Indices

Usama Afzal*
School of Microelectronics, Tianjin University, Tianjin 300072 - China



## Abstract

This study analyzes X-ray diffraction (XRD) patterns of graphene, graphene oxide, and reduced graphene oxide, identifying key crystallographic planes and their corresponding interplanar spacing through Miller indices. Graphene exhibits peaks for (002) and (004) planes, while graphene oxide shows peaks for (001) || (004) ⊥ (100) planes. Reduced graphene oxide has peaks for (002) and (001) planes. All findings are visually represented with unit cells, providing a valuable educational tool for understanding XRD patterns and the structure of the graphene family.

**Keywords:** Diffraction, miller indices, unit cell, planes direction



**How to cite:**
Afzal, U. (2024). A Comprehensive Tutorial on Graphene Family X-ray Diffraction Analysis: Graphical Representation of Miller Indices . *Siazga Research Journal, 3(2),* 96 -105.
**https://doi.org/10.58341/srj.v3i2.54**

## 1. INTRODUCTION

X-ray diffraction (XRD) is a technique in material science used to structurally characterize a material by observing the molecular and atomic structure of that material [1-5]. For this purpose, the sample of a material is irradiated with incident monochromatic light (X-rays) and the scattering angle with respect to intensities of light which is scattered by the atomic structure of the material [6]. Then a plot is drawn between the intensity of the scattered X-rays and the scattering angle for observing the material structure by analyzing an XRD pattern (which is based on scattering angle, intensity peaks with their location) and the intensities of scattered intensity peaks). Through the XRD pattern, one can get identification of the crystalline phase of the material (material name), the order of peaks, and the number of matched and unmatched peaks with the ideal one. This means XRD also gives information about the structure deviating from the ideal one due to defects and internal stress. XRD is based on Bragg's law [7-9] i.e. when the X-ray is incident on a crystal with some angle 'θ', reflects with the same scattering angle and if the d-space is equal to the wavelength of X-ray 'λ', then there occurs constructive interference. So Bragg's equation [10, 11] is written as:

$$n\lambda = 2d_{hkl}\sin\theta \qquad (1)$$

Here 'λ' is the wavelength of the incident light; 'θ' is the angle and 'd_hkl' is the space between planes with the Miller Indices (hkl). Also 'n' is an integer number which is representing the diffraction harmonic order. According to the above equation, when an X-ray beam incident on a crystal it is diffracted by the internal atoms/molecules and scattered in a specific direction as can be seen in Figure 1. The scattered X-ray light produces a spectrum of high and low intensities due to the interference (which occurs due to the diffraction of light by internal atoms). The scattering of X-ray light can be found by the electron

*Corresponding Author: Usama Afzal, School of Microelectronics, Tianjin University - Pakistan
mohammadusamafzal7@gmail.com

density of the crystal [12]. Similarly, for scattering intensity, one can consider the following reference [13].

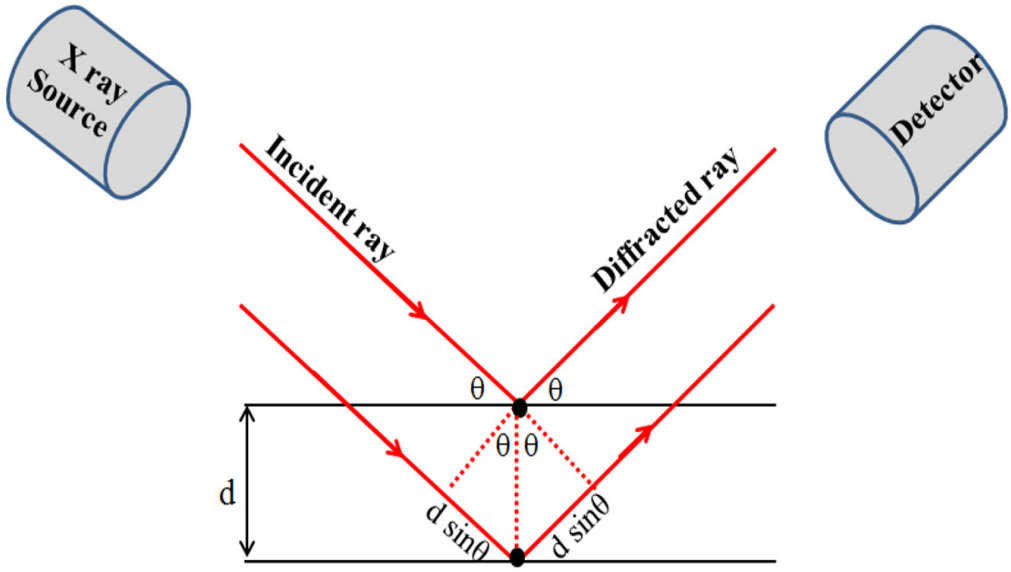


**Figure 1:** X-ray diffraction: implementation of Bragg's law

Now, let us move to the Miller Indices. Miller indices are used to specify the direction and plane in crystals or lattices with three integers 'h', 'k' and 'l' [14]. These are denoted as (hkl) for plane and [hkl] for direction which is orthogonal to reciprocal lattices, as shown in the following formula:

$$g_{hkl} = hb_1 + kb_2 + lb_3 \qquad (2)$$

Here 'b_i' represent the basis of reciprocal lattices. For cubic structure simply miller indices are used [15], so the d spacing between lattices plane with lattices constant 'a' can be measured by the following formula:

$$d_{hkl} = \frac{a}{\sqrt{h^2+k^2+l^2}} \qquad (3)$$

Similarly, for 2D hexagonal structure same indices (hkl) are used but for 3D hexagonal structure four indices (hkl) are used [16]. However, the d spacing between lattices plane with lattices constant 'a' can be measured by the following formula:

$$d_{hkl} = \frac{a}{\sqrt{\frac{4}{3}(h^2+k^2+hk)+\frac{a^2}{c^2}l^2}} \qquad (4)$$

Nowadays different two-dimensional and three-dimensional materials as well as their composite materials are used in the fabrication of different devices like energy conversions, sensors and other electric devices [17-20]. Graphene is a well-known two-dimensional material with a hexagonal structure [21], which has been paid heed by researchers. Due to the remarkable structure, electric and thermal properties of graphene it is used in the fabrication of different devices [22-25], also researchers have used graphene composite with other organic and inorganic materials. Moreover, researchers have also worked on the fabrication of 3D graphene/graphene foam based on Ni foam and other materials [26-30].

This study aimed to elucidate the crystallographic structure of graphene, graphene oxide, and reduced graphene oxide using X-ray diffraction (XRD) analysis. By correlating the XRD patterns with the material's lattice structure and employing Miller indices, the research identified key crystallographic planes and their corresponding interplanar spacing (d-spacing) for each material. The findings are visually represented with unit cells for a clear understanding, offering a valuable educational tool for researchers and students studying the structure of the graphene family through XRD techniques.

### X-ray Diffraction Analysis

Now let us discuss the x-ray diffraction pattern of the graphene family i.e. graphene, graphene oxide and reduced graphene oxide with the miller indices of lattices.

### Graphene XRD Analysis

Graphene is the 2D allotropic form of carbon and all carbon atoms have a uniform honeycomb planar arrangement. The distance between atoms is about 'i = 1.42 Å' [31] as shown in Figure 2. All carbon atoms have a linear combination of a single s-orbital with two p-orbitals i.e. sp2 hybridization. That's why a single carbon atom has chemical bonding (covalent bond) with three neighbouring atoms having an angle of 120o. Similarly from the figure, a unit cell with lattice constant 'a = 2.46 Å' can be seen. The unit cell is represented through two vectors 'a' and 'b'.

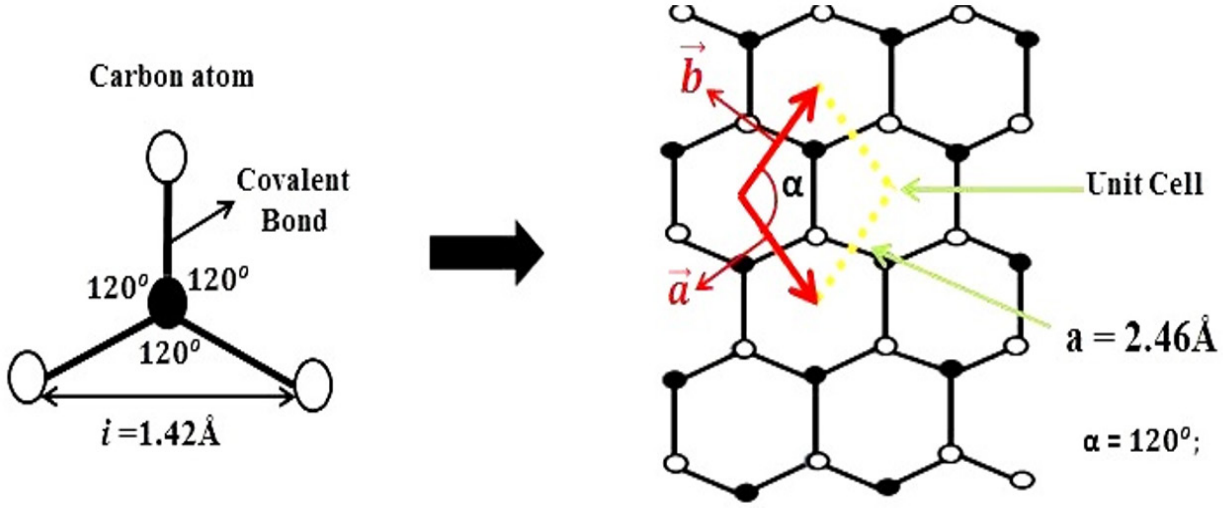


**Figure 2:** Lattices representation of graphene atomic structure with unit cell

The XRD pattern of graphene is shown in Figure 3. According to my best, it is observed that most researchers got a sharp peak at (002) and a small peak at (004) [32, 33]. However, there may be a slight change in angle. For example, (Johra, F. T. et al, 2014) observed a (002) peak at about 2θ = 25o with d-spacing 3.56 Å (They got a broadening peak for graphene at (002), so read the graph with a graph reader and approximate the angle for it) [32]. Moreover, (Aziz, M. et al, 2014) reported (002) graphene peak at 2θ = 26.4o with d-spacing 3.373 Å [34]. Similarly, (SIBURIAN, R. et al, 2018) observed (002) peak at 2θ = 23.88o angle with d-space 3.72 Å [33]. Let us see the XRD of graphene which is observed through the Cu Kα X-ray source (having a wavelength of 1.542 Å [35]).

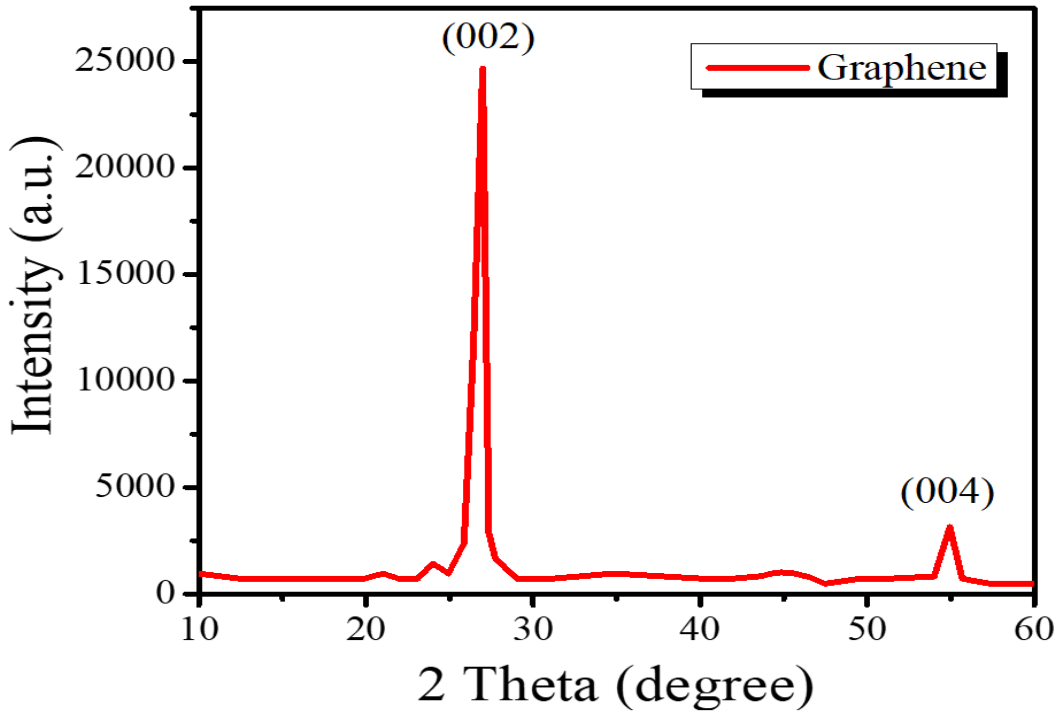


**Figure 3:** XRD pattern of graphene

The XRD pattern expresses two peaks one is (002) at 2θ = 26.98o and the other is (004) at 2θ = 54.93o. The d-space for both peaks has been measured through Bragg's formula which is d002 = 3.305 Å and d004 = 1.699 Å. The diffraction of X-rays from planes 002 and 004 can be seen in Figure 4.

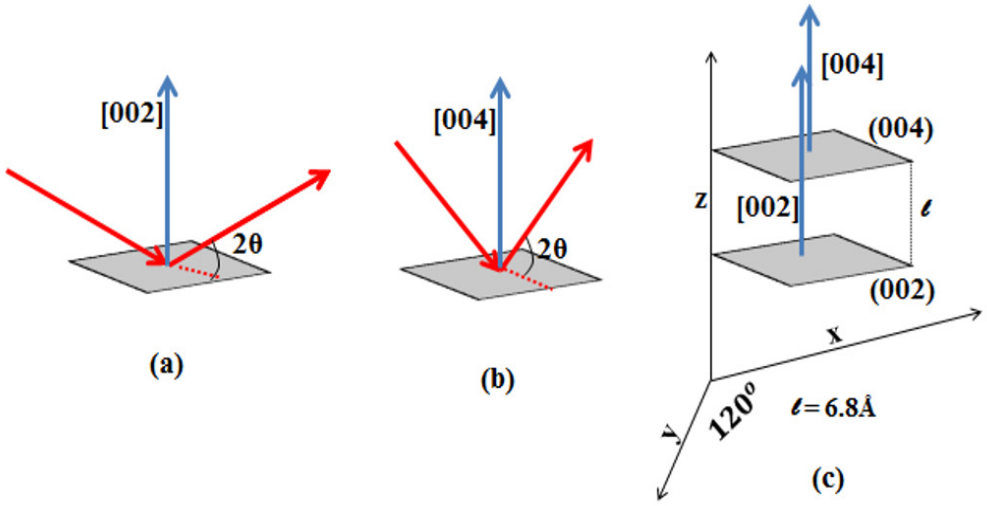


**Figure 4:** (a) X-ray diffraction for miller indices (002), (b) X-ray diffraction for miller indices (004) and (c) two parallel planes

Figure 4 (a, b & c) represents the graphical diffraction of Cu Kα X-ray from the (002) and (004) planes, respectively. It can be observed that at 2θ = 26.98o Bragg's law is fulfilled for the (002) plane with d002 = 3.305 Å and [002] plane direction. So, a sharp peak of X-ray is observed for the (002) plane. (004) plane is parallel to the (002) plane with the distance between both being l = 6.8Å [36, 37], but for the plane (004) a small peak has been observed at 2θ = 53.98o with d004 = 1.699 Å and [004] plane direction. This is because the (004) plane has half d-spacing as the (002) plane i.e. d_004= 1/2 d_002. The XRD pattern peaks are similar to the graphite peaks. Moreover, the planes of graphene are similar to the basal planes of graphite [38]. Which is indicating that there is still retained the atomic or molecular structure of carbon by graphene. But the peaks are weakened than graphite [39]. Because the layer size of graphene is smaller as compared to graphite [40].

### Graphene Oxide XRD Analysis

The structure of graphene oxide (GO) is similar to graphene as graphene oxide is a chemical modification of graphene. However, GO has some bonding with the oxygen groups [41]. It is a single-layer material (maybe multi-layers [42]) that is made of carbon, hydrogen and oxygen molecules i.e. carboxylic acid at the edges and phenol hydroxyl and epoxide groups on the basal plane [43, 44] as shown in Figure 5. As graphene oxide is the multi-layers of graphene, the unit cell and lattices constant are the same as graphene.

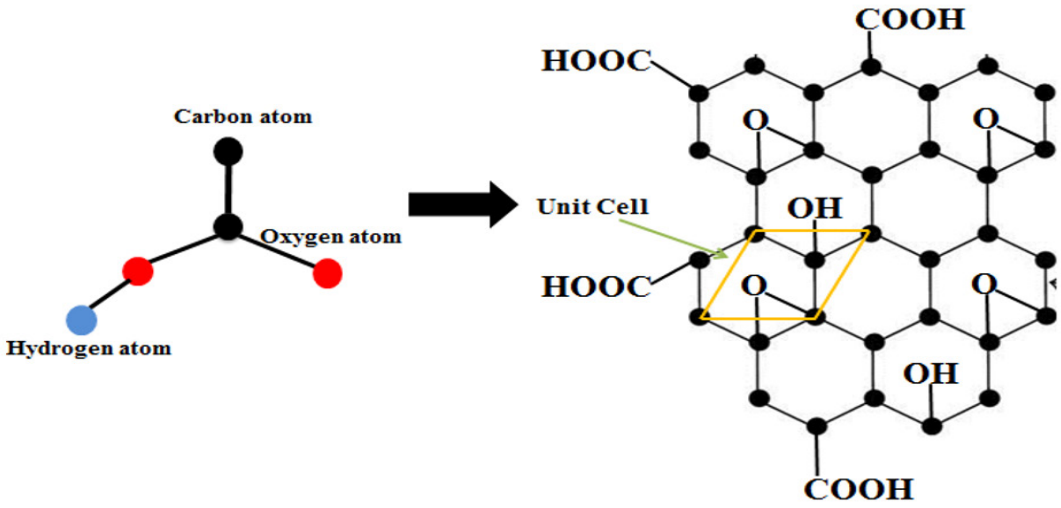


**Figure 5:** Structure of graphene oxide

The XRD pattern of graphene is shown in Figure 6. According to my best, it is observed that most research got a sharp peak at (001) [45, 46], a small peak at (100) [32, 47-49] and (004) [50]. However, there may be a slight change in angle. Let us see the XRD of graphene oxide which is observed through the Cu Kα X-ray source (having a wavelength of 1.542 Å [35].

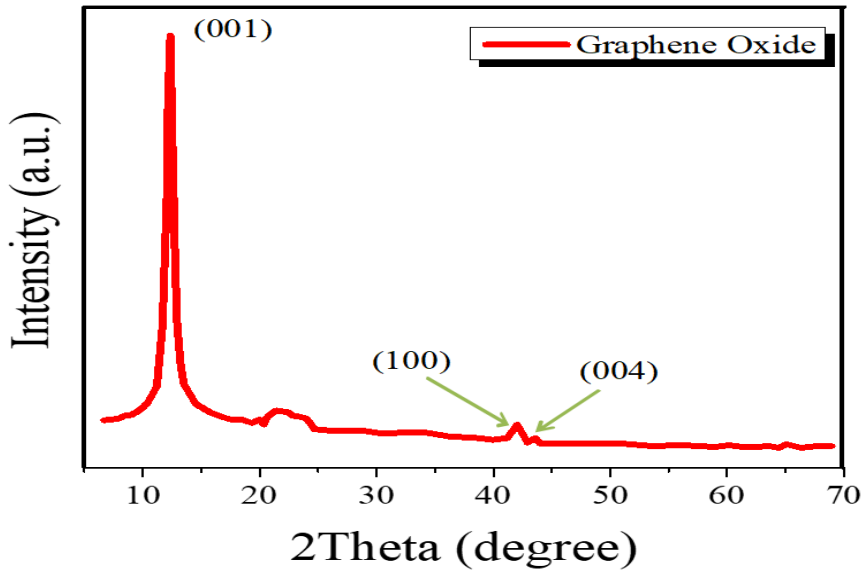


Φιγυρε 6: XRD pattern of graphene oxide

The XRD pattern expresses three peaks one is (001) at 2θ = 11.01o, the second is (100) at 2θ = 42.93o and the third is (004) at 44.04o. The d-space for both peaks has been measured through Bragg's formula which is d001 = 8.116 Å, d100 = 2.106 Å and d004 = 2.029 Å. The diffraction of X-rays from planes 001, 100 and 004 can be seen in Figure 7.

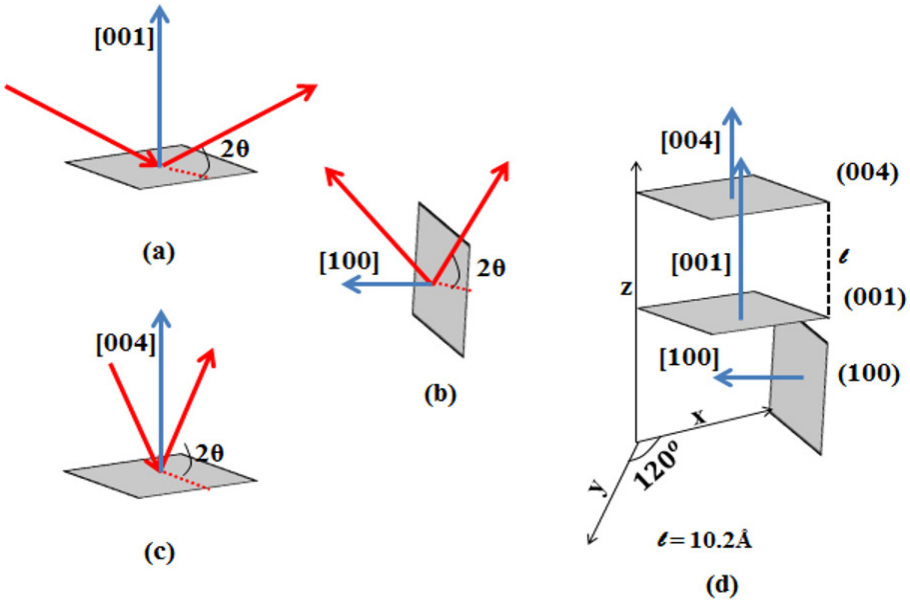


**Figure 7:** (a) X-ray diffraction for miller indices (001), (b) X-ray diffraction for miller indices (100), (c) X-ray diffraction for miller indices (100) and (d) Combine planes

Figure 7 (a, b, c & d) represents the graphical diffraction of Cu Kα X-ray from the (001), (100) and (004) planes of graphene oxide, respectively. It can be observed that at 2θ = 11.01o Bragg's law is fulfilled for (001) plane with d001 = 8.116 Å and [001] plane direction. So, a sharp peak of X-ray is observed for the (001) plane. (004) plane is parallel to the (001) plane with the distance between both being l = 10.2Å [36, 37], but for the plane (004) a small peak has been observed at 2θ = 44.04o with d004 = 2.029 Å and [004] plane direction. This is because the (004) plane has one-fourth d-spacing than the (001) plane i.e. d_004= 1/4 d_002. However, (100) is the perpendicular plane with (001) and (004). The plane diffracts the X-ray

at 2θ = 42.93o, but does not produce a sharp peak due to its alinement. The XRD of graphene oxide is similar to the XRD of graphite oxide. However, the layer size of graphene oxide is smaller compared to graphite oxide [33].

**Reduced Graphene Oxide XRD Analysis**

Reduced graphene oxide (rGO) is a form of graphene oxide which is synthesized through chemical, thermal, physical and other methods by reducing the oxygen from graphene oxide [51]. To obtain the graphene this reducing process is used and removes the oxidized functional groups from graphene oxide [52, 53] as shown in Figure 8. However, the oxygen is not removed completely, there exists a bit of oxygen atoms and functional groups i.e. there are always some defects [54-56].

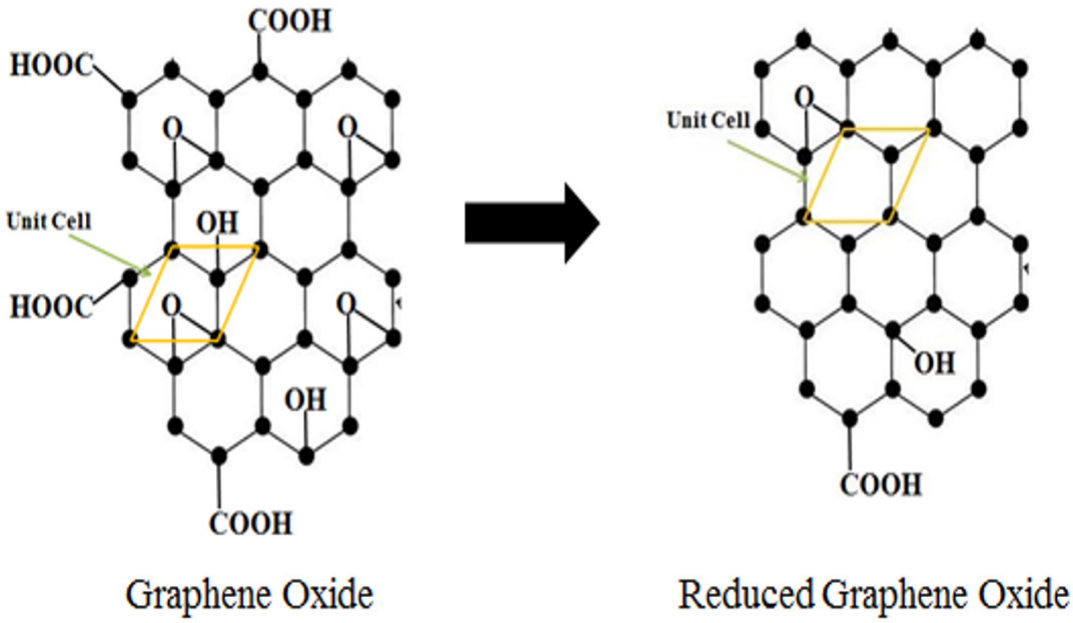


Φιγυρε 8: Structure of reduced graphene oxide

The XRD pattern of reduced graphene oxide is shown in Figure 9. According to my best, it is observed that most researchers got a sharp peak at (002) and a small peak at (001) [22, 57, 58]. Similarly, some researchers also have observed a sharp peak at (100) as can be seen in the following reference [58]. Let us see the XRD of reduced graphene oxide which is observed through the Cu Kα X-ray source (having a wavelength of 1.542 Å [35]).

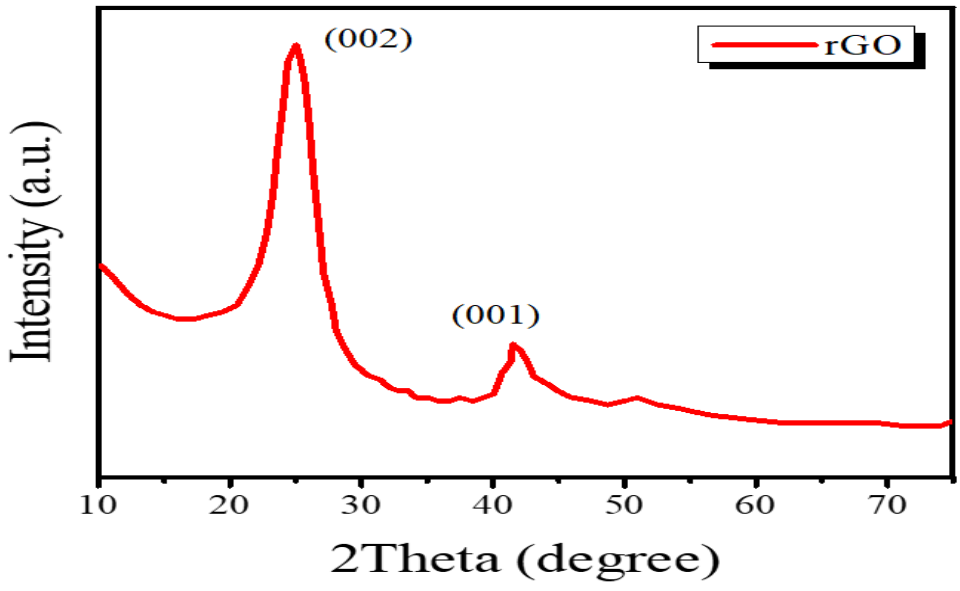


**Figure 9:** XRD pattern of graphene oxide

The XRD pattern expresses two peaks one is (002) at 2θ = 25.03o and the other is (001) at 41.50o. The d-space for both peaks has been measured through Bragg's formula which is d002 = 3.558 Å and d001 = 2.176 Å. The diffraction of X-rays from planes 002 and 001 can be seen in Figure 10.

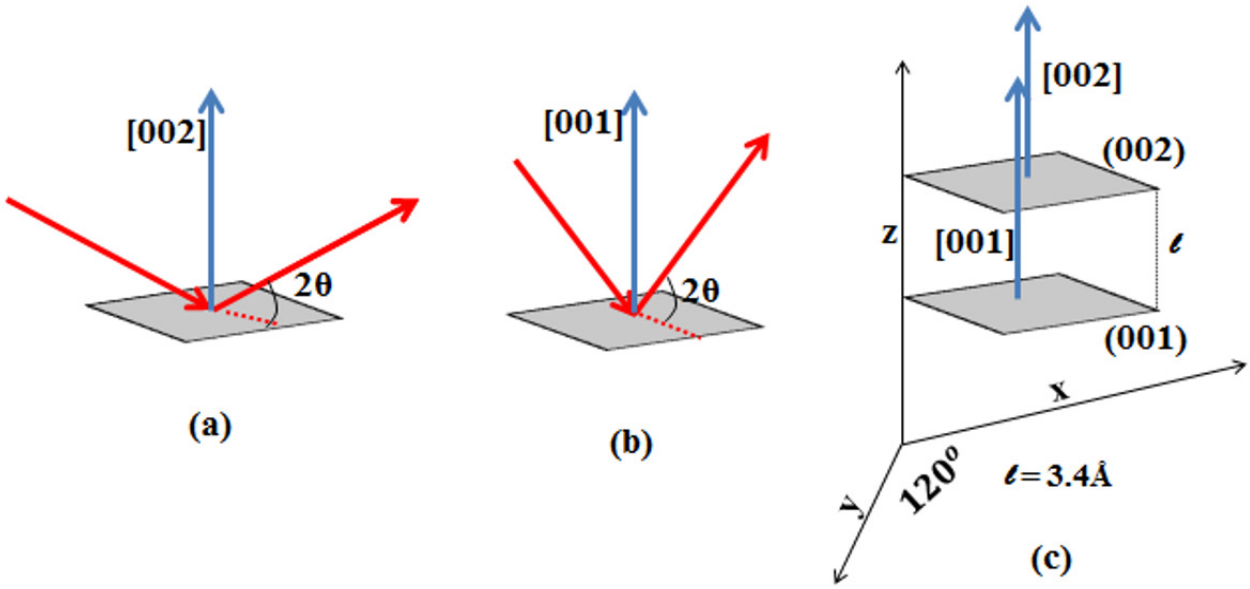


**Figure 10**: (a) X-ray diffraction for miller indices (002), (b) X-ray diffraction for miller indices (004) and (c) two parallel planes

Figure 10 (a, b & c) represents the graphical diffraction of Cu Kα X-ray from the (002) and (001) planes, respectively. It can be observed that at 2θ = 25.03o Bragg's law is fulfilled for (002) plane with d002 = 3.558 Å and [002] plane direction. So, first, a sharp peak of X-ray is observed for the (002) plane like graphene. This is expressing the presence of graphene [59]. The (001) plane is parallel to the (002) plane with the distance between both being l = 3.4Å [36, 37]. But for the plane (001) a small peak has been observed at 2θ = 41.50o with d001 = 2.176 Å and [001] plane direction. This is because the (001) plane has a smaller d-spacing than the (002) plane. In addition, the peak of (001) is observed after the plane (002) due to the disorder in the turbostratic band of carbon material [60].

## 2. CONCLUDING REMARKS

This study reviews the crystallographic structure of graphene, graphene oxide, and reduced graphene oxide using X-ray diffraction (XRD) analysis. By correlating the XRD patterns with the material's lattice structure and employing Miller indices, the research identified key crystallographic planes and their corresponding interplanar spacing (d-spacing) for each material. Graphene exhibits peaks for (002) and (004) planes, while graphene oxide shows peaks for (001) || (004) ⊥ (100) planes. Reduced graphene oxide has peaks for (002) and (001) planes. All findings are visually represented with unit cells, providing a valuable educational tool for understanding XRD patterns and the structure of the graphene family. It's important to acknowledge that X-ray diffraction analysis has limitations, such as difficulty in determining the atomic arrangement within the layers and potential ambiguity in assigning peaks for highly similar d-spacing values. However, this study offers a clear and foundational understanding of the crystallographic planes in these materials.

### Competing Interests

The author did not declare any competing interest.

## References

Afzal, U., et al., *Use of highly sensitive nickel phthalocyanine based humidity sensor to explore the imprecise data analysis for robot body.* Sensor Review, 2023(ahead-of-print).

Ahmed, N., et al., *Structural, Optical, and Magnetic Properties of Pure and Ni–Fe-Codoped Zinc Oxide Nanoparticles Synthesized by a Sol–Gel Autocombustion Method.* ACS omega, 2023. **9**(1): p. 137-145.

Shafiq, F., et al., *Development of highly sensitive relative humidity sensor based on nanoporous PCPDTBT thin film.*

Synthetic Metals, 2023. **298**: p. 117429.

Farooq, Z., et al., *Investigation of relative humidity-sensing performance of capacitive and resistive type sensor based on TDTBPPNi metalloporphyrin dielectric layer.* Bulletin of Materials Science, 2021. **44**: p. 1-10.

Afzal, U., et al., *Fabrication and characterization of a highly sensitive and flexible tactile sensor based on indium zinc oxide (IZO) with imprecise data analysis.* ACS omega, 2022. **7**(36): p. 32569-32576.

Bunaciu, A.A., E.G. UdriŞTioiu, and H.Y. Aboul-Enein, *X-ray diffraction: instrumentation and applications.* Critical reviews in analytical chemistry, 2015. **45**(4): p. 289-299.

Chung, F.H., *Quantitative interpretation of X-ray diffraction patterns of mixtures. III. Simultaneous determination of a set of reference intensities.* Journal of Applied Crystallography, 1975. **8**(1): p. 17-19.

Copeland, L.E. and R.H. Bragg, *Quantitative X-ray diffraction analysis.* Analytical Chemistry, 1958. **30**(2): p. 196-201.

Chung, F.H., *Quantitative interpretation of X-ray diffraction patterns of mixtures. II. Adiabatic principle of X-ray diffraction analysis of mixtures.* Journal of Applied Crystallography, 1974. **7**(6): p. 526-531.

Pope, C.G., *X-ray diffraction and the Bragg equation.* Journal of chemical education, 1997. **74**(1): p. 129.

Stanjek, H. and W. Häusler, *Basics of X-ray Diffraction.* Hyperfine interactions, 2004. **154**(1): p. 107-119.

Kirfel, A., et al., *Electron density distribution and bond critical point properties for forsterite, Mg2 SiO4, determined with synchrotron single crystal X-ray diffraction data.* Physics and chemistry of minerals, 2005. **32**(4): p. 301-313.

Cattani, M., *XR ay Scattering by Atoms: Basic Equations*. 2011, Institute of Physics, University of.

Sun, S., et al., *Identification of the Miller indices of a crystallographic plane: a tutorial and a comprehensive review on fundamental theory, universal methods based on different case studies and matters needing attention.* Nanoscale, 2020. **12**(32): p. 16657-16677.

Nakagawa, S.T., *Crystallographic analysis of structural changes in cubic crystals.* Journal of the Physical Society of Japan, 2007. **76**(3): p. 034603-034603.

Ding, B., et al., *Gold film-terminated 3-dimensional photonic crystals.* Applied Physics A, 2011. **103**(3): p. 889-894.

Zhou, Y., et al., *High-efficiency organic solar cells based on a low-cost fully non-fused electron acceptor.* Advanced Functional Materials, 2021. **31**(27): p. 2101742.

Lee, K.S. and H.T. Jeong, *Development and optimization of ionic liquid based gel polymer electrolyte for all solid-state supercapacitor.* Journal of Energy Storage, 2021. **42**: p. 103001.

Liu, J., et al., *A study of low-temperature solid-state supercapacitors based on Al-ion conducting polymer electrolyte and graphene electrodes.* Journal of Power Sources, 2021. **488**: p. 229461.

Afzal, U., et al., *Fabrication of a surface type humidity sensor based on methyl green thin film, with the analysis of capacitance and resistance through neutrosophic statistics.* RSC advances, 2021. **11**(61): p. 38674-38682.

Zhen, Z. and H. Zhu, *Structure and properties of graphene*, in *Graphene*. 2018, Elsevier. p. 1-12.

Afzal, U., et al., *Fabrication of flexible temperature sensors to explore indeterministic data analysis for robots as an application of Internet of Things.* RSC Advances, 2022. **12**: p. 17138-17145.

Wang, C., et al., *Flexible supercapacitors based on graphene/boron nitride nanosheets electrodes and PVA/PEI gel electrolytes.* Materials, 2021. **14**(8): p. 1955.

Eryiğit, M., et al., *Efficient CdS quantum dot sensitized solar cells based on electrochemically reduced graphene oxide (ERGO)/ZnO nanowall photoanodes and MoS2, WS2, CuS cascaded counter electrodes.* Solar Energy, 2022. **234**: p. 348-359.

Afzal, U., et al., *Fabrication of a graphene-based sensor to detect the humidity and the temperature of a metal body with imprecise data analysis.* RSC advances, 2022. **12**(33): p. 21297-21308.

Afzal, U., M. Aslam, and A.H. Al-Marshadi, *Analyzing imprecise graphene foam resistance data.* Materials Research Express, 2022.

Saeed, G., et al., *Metal-organic framework-derived (Mn-1) CoxSy@(Ni–Cu) OHs marigold flower-like core@ shell as cathode and (Mn–Fe10) Sx@ graphene–foam as anode materials for ultra-high energy-density asymmetric supercapacitor.*

Materials Today Chemistry, 2022. **23**: p. 100758.

Zhu, J., et al., *Cu/CuO-Graphene Foam with Laccase-like Activity for Identification of Phenolic Compounds and Detection of Epinephrine*. Chemical Research in Chinese Universities, 2022: p. 1-9.

Huang, Z., et al., *Hierarchical nanostructure of three-dimensional Au/carbon nanotube-graphene foam for high performance lithium metal anode*. Solid State Ionics, 2022. **380**: p. 115941.

Afzal, U., et al., *Fabrication of graphene-based sensor for exposure to different chemicals*. RSC advances, 2022. **12**(52): p. 33679-33687.

Koehler, F.M. and W.J. Stark, *Organic synthesis on graphene*. Accounts of chemical research, 2013. **46**(10): p. 2297-2306.

Johra, F.T., J.-W. Lee, and W.-G. Jung, *Facile and safe graphene preparation on solution based platform*. Journal of Industrial and Engineering Chemistry, 2014. **20**(5): p. 2883-2887.

Siburian, R., et al., *New route to synthesize of graphene nano sheets*. Oriental Journal of Chemistry, 2018. **34**(1): p. 182.

Aziz, M., F.S.A. Halim, and J. Jaafar, *Preparation and characterization of graphene membrane electrode assembly*. Jurnal teknologi, 2014. **69**(9).

Jenkins, R. and J.L. De Vries, *Practical X-ray spectrometry*. 1970: Macmillan International Higher Education.

Popov, A.M., et al., *AA stacking, tribological and electronic properties of double-layer graphene with krypton spacer*. The Journal of chemical physics, 2013. **139**(15): p. 154705.

De Andres, P., R. Ramírez, and J.A. Vergés, *Strong covalent bonding between two graphene layers*. Physical Review B, 2008. **77**(4): p. 045403.

Velický, M.j., et al., *Electrochemistry of the basal plane versus edge plane of graphite revisited*. The Journal of Physical Chemistry C, 2019. **123**(18): p. 11677-11685.

Wang, X. and L. Zhang, *Green and facile production of high-quality graphene from graphite by the combination of hydroxyl radicals and electrical exfoliation in different electrolyte systems*. RSC advances, 2019. **9**(7): p. 3693-3703.

Ma, W., J. Zhou, and S. Cheng, *Preparation and characterization of graphene*. Journal of Chemical Engineering of Chinese Universities, 2010. **24**(4): p. 719-722.

Jianguo, S., W. Xinzhi, and C. Chang-Tang, *Preparation and characterization of graphene oxide*. J. Nano. Mater, 2014.

Suarez-Martinez, I., N. Grobert, and C. Ewels, *Nomenclature of sp2 carbon nanoforms*. Carbon, 2011. **50**: p. 741-747.

Ray, S.C., *Application and uses of graphene oxide and reduced graphene oxide*. Applications of graphene and graphene-oxide based nanomaterials, 2015. **1**.

Raidongia, K., A.T. Tan, and J. Huang, *Graphene oxide: some new insights into an old material*, in *Carbon nanotubes and graphene*. 2014, Elsevier. p. 341-374.

Yasin, G., et al., *Exploring the nickel–graphene nanocomposite coatings for superior corrosion resistance: manipulating the effect of deposition current density on its morphology, mechanical properties, and erosion-corrosion performance*. Advanced Engineering Materials, 2018. **20**(7): p. 1701166.

Aliyev, E., et al., *Structural characterization of graphene oxide: Surface functional groups and fractionated oxidative debris*. Nanomaterials, 2019. **9**(8): p. 1180.

Ain, Q.T., et al., *The systemic effect of PEG-nGO-induced oxidative stress in vivo in a rodent model*. Beilstein journal of nanotechnology, 2019. **10**(1): p. 901-911.

Aragaw, B.A., *Reduced graphene oxide-intercalated graphene oxide nano-hybrid for enhanced photoelectrochemical water reduction*. Journal of Nanostructure in Chemistry, 2020. **10**(1): p. 9-18.

Ban, F., et al., *Graphene oxide and its electrochemical performance*. Int. J. Electrochem. Sci, 2012. **7**(5): p. 4345-4351.

Abdelaal, S., et al., *The physical structure and surface reactivity of graphene oxide*. Diamond and Related Materials, 2020. **101**: p. 107613.

Papageorgiou, D.G., I.A. Kinloch, and R.J. Young, *Graphene/elastomer nanocomposites*. Carbon, 2015. **95**: p. 460-484.

Quezada-Renteria, J.A., et al., *Influence of protons on reduction degree and defect formation in electrochemically reduced*

*graphene oxide*. Carbon, 2019. **149**: p. 722-732.

Moon, I.K., et al., *Reduced graphene oxide by chemical graphitization*. Nature communications, 2010. **1**(1): p. 1-6.

Eigler, S., C. Dotzer, and A. Hirsch, *Visualization of defect densities in reduced graphene oxide.* Carbon, 2012. **50**(10): p. 3666-3673.

Rozada, R., et al., *Towards full repair of defects in reduced graphene oxide films by two-step graphitization*. Nano Research, 2013. **6**(3): p. 216-233.

Compton, O.C. and S.T. Nguyen, *Graphene oxide, highly reduced graphene oxide, and graphene: versatile building blocks for carbon-based materials.* small, 2010. **6**(6): p. 711-723.

Liu, G., et al., *A reduced graphene oxide modified metallic cobalt composite with superior electrochemical performance for supercapacitors.* RSC Advances, 2015. **5**(78): p. 63553-63560.

Hidayah, N., et al. *Comparison on graphite, graphene oxide and reduced graphene oxide: Synthesis and characterization*. in *AIP Conference Proceedings*. 2017. AIP Publishing LLC.

Cui, P., et al., *One-pot reduction of graphene oxide at subzero temperatures.* Chemical Communications, 2011. **47**(45): p. 12370-12372.

Low, F.W., C.W. Lai, and S.B. Abd Hamid, *Easy preparation of ultrathin reduced graphene oxide sheets at a high stirring speed.* Ceramics International, 2015. **41**(4): p. 5798-5806.